Temperature case studies in grinding including an inclined heat source model

W B Rowe
School of Engineering, Liverpool John Moores University, Byrom Street, Liverpool L3 3AF, UK

Abstract: Previous analytical models of heat transfer in grinding have been based on the sliding heat source analysed by Jaeger and Carslaw in 1942. It is now shown that for deep grinding processes, and particularly for high efficiency deep grinding (HEDG), the sliding model overestimates the temperatures experienced by the finished workpiece surface. These situations are re-analysed using sliding sources and inclined sources to estimate contact surface temperatures and subsurface temperatures in grinding. Convection in the abrasive contact region to the process fluid, to the grinding wheel and to the chip material removed is taken into account. It is shown that each of these effects can predominate under different process conditions. Case studies illustrate the importance of thermal processes in achieving efficient material removal. The results for HEDG are particularly interesting and suggest that under the right conditions specific energy may be self-limiting. This is offered as a possible explanation for the efficiency of the process.

Keywords: grinding, temperatures, abrasive processes, high efficiency deep grinding, creep grinding

NOTATION

a	coordinate of position along the heat source
a_e	real depth of cut
b_w, b_c	width of contact
c	mean specific heat capacity
C	temperature constant
d_e	effective wheel diameter
e_c	specific energy
e_{ch}	specific energy to chips
h_f	workpiece–fluid convection coefficient
h_w	workpiece conduction coefficient
k	thermal conductivity
$K_0(u)$	Bessel function of second kind, order zero
l_c	contact length
Pe	Peclet number
q	heat flux (rate of heat per unit area)
q_{ch}	energy to chips represented as a heat flux
q_f	energy to fluid represented as a heat flux
q_t	total heat flux generated in the contact area
q_w, q_0	average heat flux entering the workpiece surface
q_{ws}	energy to workpiece and grains represented as a heat flux
Q_w	workpiece removal rate
Q'_w	workpiece removal rate per unit width of contact
r_0	equivalent contact radius of the abrasive grains
R_c	proportion of the grinding energy convected by the chips
R_f	proportion of the grinding energy convected by the fluid
R_s	proportion of the grinding energy conducted into the abrasive grains
R_w	proportion of grinding energy conducted into the workpiece
R_{ws}	workpiece–grain partition ratio
t	time coordinate
t_c	contact time between wheel and point on workpiece
T	temperature
T_{av}	average workpiece background temperature in the contact zone
T_{max}	maximum workpiece background temperature
T_{mp}	melting point temperature of workpiece material
T_w	workpiece background temperature
T_{wg}	spike temperature between workpiece and grain
v	linear speed of a moving heat source
v_s	wheel speed
v_w	work speed
x	coordinate parallel to work speed direction
z	coordinate normal to work speed direction
α	thermal diffusivity
β	thermal property $= \sqrt{k\rho c}$
ϕ	inclination angle of heat source plane

The MS was received on 21 December 1999 and was accepted after revision for publication on 28 July 2000.

1 INTRODUCTION

Well-designed abrasive machining processes usually enhance workpiece surface quality, producing low roughness, compressive or neutral residual stresses and improved fatigue life. Conversely, abusive machining leads to a range of forms of surface damage. Mostly, the higher is the temperature when machining hardened steels, the greater is the damage caused to the surface. Potential forms of damage include softening of hardened surfaces, rehardening, tensile stresses, cracking, oxidation, wheel loading, high forces, poor surface texture and vibrations

In this paper, consideration is given to the relationships between process energy, selection of grinding conditions and thermal aspects of process design to achieve high productivity and surface integrity. A more accurate model of conduction into the workpiece for deep cuts is introduced based on the moving inclined heat source instead of the sliding heat source used by previous researchers.

Thermal analysis has greatly clarified the importance of the various physical processes involved in abrasive machining processes leading to radical developments such as creep grinding and high efficiency deep grinding (HEDG). The following analysis is therefore justified in terms of the benefits obtainable with an integrated systems approach and improved process understanding.

2 KEY DEVELOPMENTS IN PREVIOUS WORK

Some findings in the development of thermal modelling are listed in Table 1. The most important of these dates back to 1942 with the sliding heat source model by Jaeger for a heat flux distributed uniformly across the grinding contact [**1**]. This model is used by most researchers up to the present day. However, to place the subject in context, some other concepts required to understand the difference between a conventional turning process and the grinding process which is closer to a micro-milling process should be looked at briefly.

Outwater and Shaw [**2**] viewed material removal in much the same way as a turning operation and modelled heat transfer to the workpiece based on a sliding heat source at the shear plane. However, with cutting edges with large negative rake angles, this assumption underestimates the proportion of the heat energy entering the workpiece. Hahn [**3**] reasoned from energy considerations that the principal heat generation is at the grain–workpiece rubbing surface. This follows because the shear plane energy assumption cannot account for the much larger energy experienced in practice. The heat energy is therefore more accurately described by considering the energy to be dissipated as heat at the contact between the workpiece and the grain, neglecting the energy dissipated as heat at the shear plane. In practice, shear plane and wear flat energies are important

Most often, the heat carried away in the chips is a small proportion of the total heat generated. Malkin [**6**] realized from a simple calculation of the melting energy of the chips that the maximum energy which could be convected by the chips was limited. For ferrous materials, this energy is approximately 6 J/mm^3. Further consideration leads to the assumption that this forms a reasonable basis for the estimation of the energy convected by the chips.

It is practically impossible to predict workpiece temperatures with any accuracy purely from theory, because actual energies depend greatly on the extent of fracture and subsurface redundant work which in turn depend on many factors including the topography of the grinding wheel and the friction conditions. The starting point for temperature prediction is therefore based in most cases on measured forces or power levels from which specific energy levels can be determined for the particular machining conditions.

Many authors have applied oversimplifications in calculating machining temperature. For example, it would be tempting to assume that all the machining energy goes into the geometric contact area of the workpiece, ignoring all other heat sinks. In general, this overestimates the surface temperatures and is quite useless for practical control of many grinding processes.

Table 1 Key developments listed by year, first author and reference

1942	Jaeger	[**1**]	Sliding heat source model
1952	Outwater	[**2**]	Shear plane energy partitioning model
1962	Hahn	[**3**]	Energy partition between grain and workpiece
1966	Makino	[**4**]	Real contact length $l_e > l_g$
1970	Des Ruisseaux	[**5**]	Fluid convection over l_e
1971	Malkin	[**6**]	Limiting chip energy and sliding energy
1975	Shafto	[**7**]	Fluid boiling and limiting fluid energy
1978	Snoeys	[**8**]	Triangular heat flux
1980	Werner	[**9**]	Wheel–work–fluid–chip partitioning
1989	Lavine	[**10**]	Conical grain (one-dimensional) model
1991	Rowe	[**11**]	Transient contact model
1993	Rowe	[**12**]	Force/contact length model
1995	Rowe	[**13**]	Critical temperatures for tempering
1996	Ueda	[**14**]	Grain temperatures
1996	Rowe	[**15**]	Effective abrasive thermal properties

Useful estimates of temperature for shallow cut grinding processes can be obtained by systematic application of the key principles listed above. However, for deep cut grinding, the sliding heat source model is an inaccurate representation of the geometry and kinematics of the process. Realistic temperature estimates are necessary to provide process understanding and process improvements.

In 1966, Makino *et al.* [**4**] measured temperatures using a thermocouple and found that the actual length of the heat source in shallow cut grinding was 2–3 times the geometric contact length. The assumption of a geometric contact length overestimates the heat flux density (that is, power/contact area) in the contact zone and as a result predicts artificially high temperatures. In 1993, Rowe and Qi [**12**] found that the contact length could be predicted on the basis of the combination of the geometric contact length and the elastic contact length due to the forces. However, in deep grinding, where the depths of cut are measured in millimetres rather than microns, the geometric contact length can be employed with little loss of accuracy.

The effect of surface cooling by a grinding fluid was analysed in 1970 by Des Ruisseaux and Zerkle [**5**]. Convective cooling in shallow grinding usually extracts less than 10 per cent of the energy within the contact zone for likely values of convection coefficients. Of course, convective cooling outside the contact region is very important for bulk cooling of the workpiece and accurate size control. The heat extracted by the fluid is later convected to the atmosphere. However, fluid cooling outside the contact region is largely ineffective in its prime function if the temperature rise within the contact region has already caused thermal damage.

In deep cut creep grinding, convective cooling inside the contact region is of much greater importance than in shallow grinding, as shown by Shafto in 1975 [**7**]. Convection is greater owing to the long arc of contact and the long contact times. In creep grinding, convective cooling sometimes extracts more heat from the contact zone than all the other elements combined. Shafto found, however, that fluid boiling limits the energy which may be extracted by fluid cooling.

Howes *et al.* [**16**] in 1987 found that fluid boiling also limits cooling and lubrication in shallow cut grinding when the temperatures in the contact zone exceed the boiling temperature of the fluid. It may therefore be concluded that the maximum energy which can be convected by the fluid is limited by the energy required to cause boiling of the fluid.

Werner *et al.* [**9**] used finite element analysis to model heat flows to the workpiece, wheel, chips and fluid in creep feed grinding. This was one of the first attempts to model the effect of all four heat sinks simultaneously. Rowe *et al.* [**17**] modelled the energy partitioning to all four heat sinks analytically. Upper and lower bound estimates of the energy to the workpiece provided confidence limits on the temperature calculations. In this early method used by Rowe *et al.*, it was assumed that a grinding wheel could be modelled as a homogeneous mass. In later papers, it was shown that it was as simple but more accurate to model the wheel as a set of discrete contacts within the contact zone based on the two-dimensional model of heat transfer into a plane grain proposed by Hahn in 1962 [**3**].

Lavine [**10**] modelled heat flows into the workpiece, the fluid and the grain using a conical grain model. The conical grain model based on a one-dimensional approximation for two-dimensional heat dispersion appears at first to give advantages over the plain grain model. However, it was later realized that the conical grain model only works for small cone angles. For larger angles typical of abrasive grains, the plane grain model is more accurate and much simpler. Rowe *et al.* [**11**] used the cone model with a more direct partitioning approach to demonstrate the effect of transient heating of the abrasive grains. It was shown that this reduces the energy partitioned to the workpiece particularly with high conductivity grains. Rowe *et al.* [**15**] demonstrated that the transient solution could also be applied to Hahn's plane grain model.

Rowe *et al.* [**13**, **18**] investigated critical temperatures for onset of thermal damage for several ferrous materials. The critical temperature for the onset of temper colours was found to lie between 450 and 500 °C under most grinding conditions. This range is higher than might be expected from heat treatment texts. The difference is due to the fact that the heat source in grinding is continually moving.

During the course of the work by Morgan *et al.* [**19**] it became apparent that the accuracies of the thermal properties of the grains were crucial to the accuracy of solutions for cubic boron nitride (CBN) grinding. This is because CBN grains are much more conductive than conventional abrasives. Large discrepancies between published values produced unacceptable uncertainties. Careful experimental work showed that it was advisable to determine effective abrasive properties from temperature measurement experiments and correlation with the thermal model to be employed. This inverse technique also calibrates out the effect of unknown factors in the system.

In this paper, the advances over many years are considered and the importance of using the inclined plane model is demonstrated for deep grinding operations. The importance of various aspects of the process is demonstrated through case studies.

3 RATE OF HEAT GENERATION

Contact temperatures are primarily dependent on the average heat flux generated in the contact zone and the duration of heating. The distribution of the heat flux is of secondary importance.

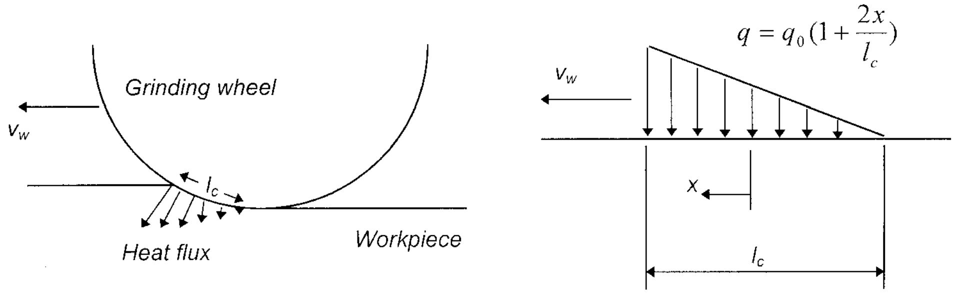

Fig. 1 The triangular heat flux assumption. The heat flux varies linearly across the contact

The rate at which energy is generated is approximately proportional to the rate of material removal. The removal rate varies almost linearly across the contact zone as in Fig. 1. The heat flux is therefore most intense at the leading edge of the contact zone as illustrated.

Early assumptions of a uniform heat distribution are not supported by temperature measurements. The potential error in the maximum temperature estimated by using the uniform heat flux distribution is an approximately 5 per cent increase. However, the positition of the maximum temperature is shifted from the exit for the uniform flux to the mid-position for the triangular flux. This is important in deep grinding for the finished workpiece surface temperature. The triangular heat distribution should be used therefore to avoid significant errors.

The average heat flux, q_0, in the contact zone is

$$q_0 = \frac{P}{l_c b_w} \tag{1}$$

where

l_c = length of the contact zone
b_w = width of the contact zone

The flux which determines the maximum temperature of the workpiece depends both on the power and also on the size of the contact zone.

The triangular flux in Fig. 1 is defined at any point x along the contact length by

$$q = q_0\left(1 + \frac{2x}{l_c}\right) \tag{2}$$

Of course, the flux described by Fig. 1 is an average of very short bursts of very intensive energy at randomly distributed small areas, where the rapidly moving grain contacts occur.

For grinding, typical durations of the heat inputs are summarized in Table 2. Each grain interaction moves past a point on the workpiece at wheelspeed so that a typical heat pulse is experienced for about 1 μs. A section of the workpiece will experience many such pulses over a much longer duration. A typical overall duration of the succession of pulses is 10 000 μs.

Table 2 Typical heating durations

Contact	Duration	Typical value
Grain at workpiece point	$2r_0/v_s$	1 μs
Grain in contact zone	l_c/v_s	100 μs
Workpiece in contact zone	l_c/v_w	10 000 μs

A grain typically moves across the whole contact length in 100 μs. The grain therefore experiences a heat pulse for a period approximately 100 times longer than the workpiece. This allows the surface of the grain to reach a steady state temperature which has been estimated to be close to the melting temperature by Ueda *et al.* [**14**].

The microsecond duration of the heat pulse due to an individual grain is too short to cause much more than a localized plastic deformation along the path of contact and localized oxidation. The effect of many such pulses averaged over a period measured in milliseconds rather than microseconds is sufficient to cause significant temperature rise at depths up to and often exceeding 0.1 mm.

In looking for the causes of surface thermal damage it is therefore necessary to be more concerned with the variation of the average heat flux according to equation (2) than with the shallow thermal damage caused by individual grains.

4 TEMPERATURES MEASURED IN SHALLOW GRINDING

Direct measurements of temperatures in abrasive machining processes are made difficult by the short duration of a large number of discrete events taking place as individual grains pass through the contact zone. Ueda *et al.* [**14**] measured the temperature of abrasive grains just after the grains left contact with the workpiece. Measurement was made by detecting infrared radiation using a fibre optic linked to a two-colour pyrometer. It was found that cooling is extremely rapid. The maximum temperature at the end of cutting diminishes to one-quarter within 1 ms. It was estimated that the maximum temperature of the grain at the end of contact is approximately equal to the melting temperature of the workpiece. This is in agreement with expectation because grinding energies greatly exceed the specific energy required to melt the material removed.

The results from Ueda *et al.* are useful, as will be described later for analysing the proportion of the energy conducted into the workpiece. However, the conclusion that the material removed reaches a temperature close to melting does not reveal much about the temperatures which give rise to thermal damage and tensile stresses. For this purpose it is necessary to measure the maximum background surface temperature of the workpiece as it moves through the contact zone.

Rowe *et al.* [**13**] used a thin foil thermocouple with a junction of 0.05 mm for discrimination of a local temperature and a fast response time. The junction is formed at the surface by the grinding action, thus allowing surface temperatures to be measured. An idealized temperature measurement is shown in Fig. 2, illustrating the difference between a 'spike' temperature, T_{wg}, experienced as an individual grain passes over the sensor and the background surface temperature, T_w.

In practice, a thermocouple is incapable of responding quickly enough to reproduce the spike temperature accurately at the workpiece–grain contact. The spike temperature is observed but attenuated. The thermocouple is, however, capable of responding to the background temperature without significant distortion. The duration of the background temperature pulse is measured in milliseconds which is sufficiently long to

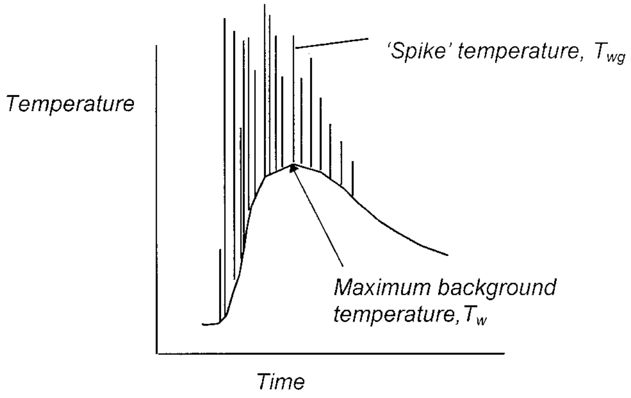

Fig. 2 Interpretation of an idealized thermocouple measurement of workpiece surface temperature

give rise to significant diffusion of heat to depths in excess of 0.1 mm.

Figure 3 shows some results when grinding an AISI 1055 steel with either a 60 grit alumina wheel or a 200 grit CBN wheel. The fine CBN wheel gives rise to higher forces and specific energy than the coarser alumina wheel but, because of the high thermal conductivity of the CBN grains, the temperatures are not increased. An important point here is that temperatures are dependent on the specific energy of the process, on the thermal properties of the abrasive and on the thermal

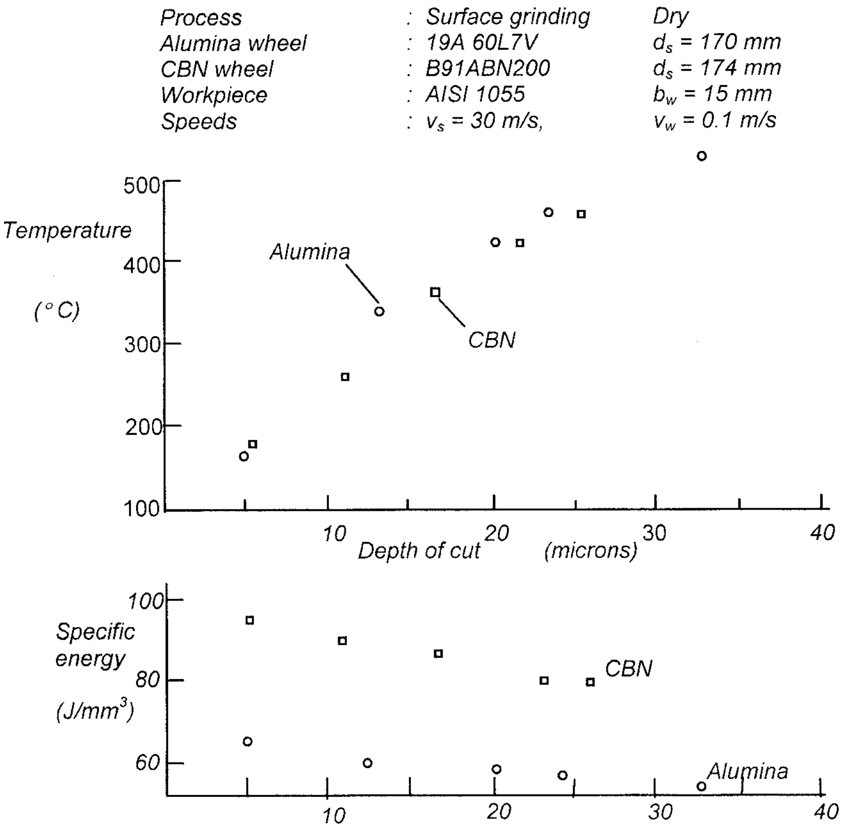

Fig. 3 Effect of depth of cut on temperature, T_{max}, for a case where the specific energy with CBN is higher than with an alumina wheel

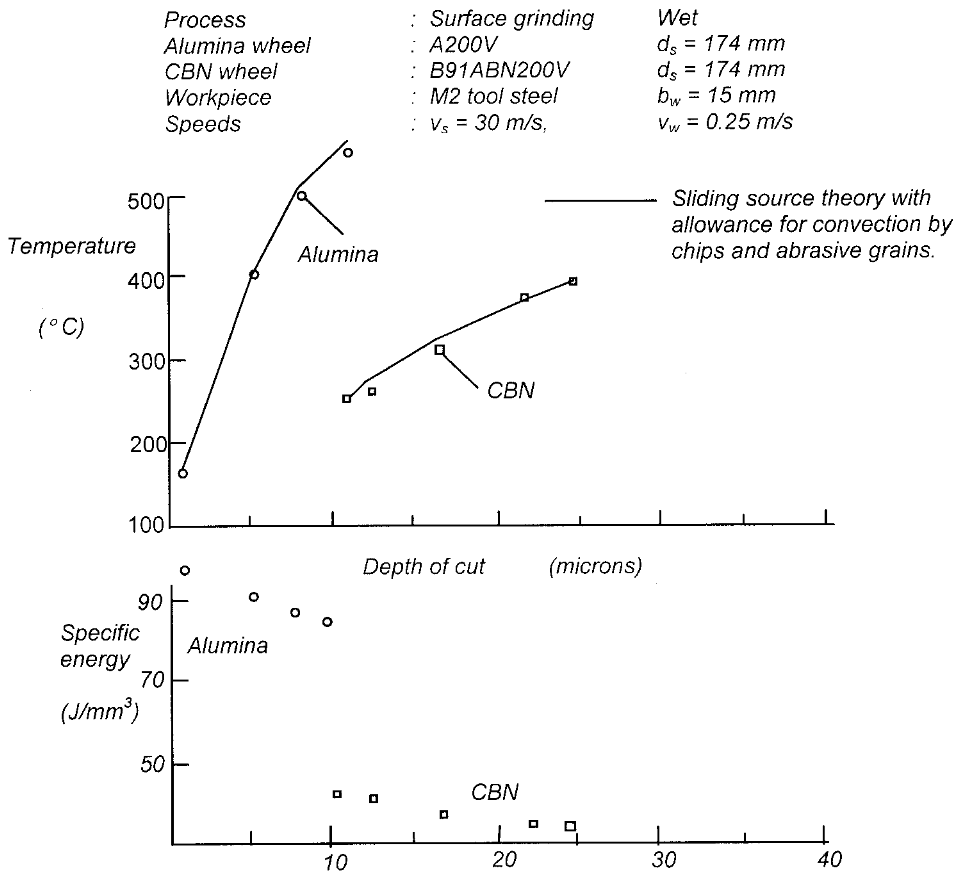

Fig. 4 Effect of depth of cut on temperature, T_{max}, for a case where the specific energy with CBN is lower than with an alumina wheel

properties of the workpiece. This point is convincingly demonstrated by contrasting the results in Fig. 3 with the results in Fig. 4. In Fig. 4, the workpiece material is M2 tool steel. In this example, the specific energy using a 200 grit CBN wheel is much lower than the specific energy using a 200 grit alumina wheel. Corresponding to the sharper condition of the CBN wheel, there is an impressive reduction in the workpiece temperature. Many such experiments confirm the validity of these conclusions.

The use of a grinding fluid can be very important for the reduction of temperatures. Figure 5 shows an example where an alumina wheel is used to grind M2 tool steel. In this example, it can be seen that a substantial reduction is achieved using a 2 per cent oil in water emulsion. The operation is shallow cut grinding so that the contact area and the contact time are relatively small and there is little scope for convective cooling in the contact zone. It can be seen that good correlation can be achieved between theory and experiment in dry and wet shallow grinding, ignoring the effects of fluid convection on the heat transfer

The main effect of the fluid on temperature is to lubricate the grinding process in shallow grinding rather than to provide convective cooling within the contact zone. The reduced specific energy is sufficient to explain the lower workpiece temperature in the above example.

A different conclusion is drawn for creep grinding where the contact area and the contact time may be 1 or 2 orders of magnitude larger than in shallow cut grinding. This is illustrated in Table 3.

Andrew *et al.* [**20**] showed that convective cooling contributes a substantial proportion of the heat dissipation in creep grinding. The success of creep grinding is strongly dependent on effective delivery of fluid into the contact zone and also on frequent or continuous dressing to maintain low values of specific energy.

At first sight, it would appear sensible to present temperature results for various process variables such as wheel speed and work speed. However, sensible interpretation of such results cannot generally be obtained without reference to the accompanying values of specific energy. This should now be clear from the above examples. To illustrate this point, consider the case where grinding wheel speed is increased. Where increased wheel speed increases specific energy, the workpiece temperature will be increased. Where increased wheelspeed reduces specific energy, the workpiece temperature will be reduced. Both situations arise in practice.

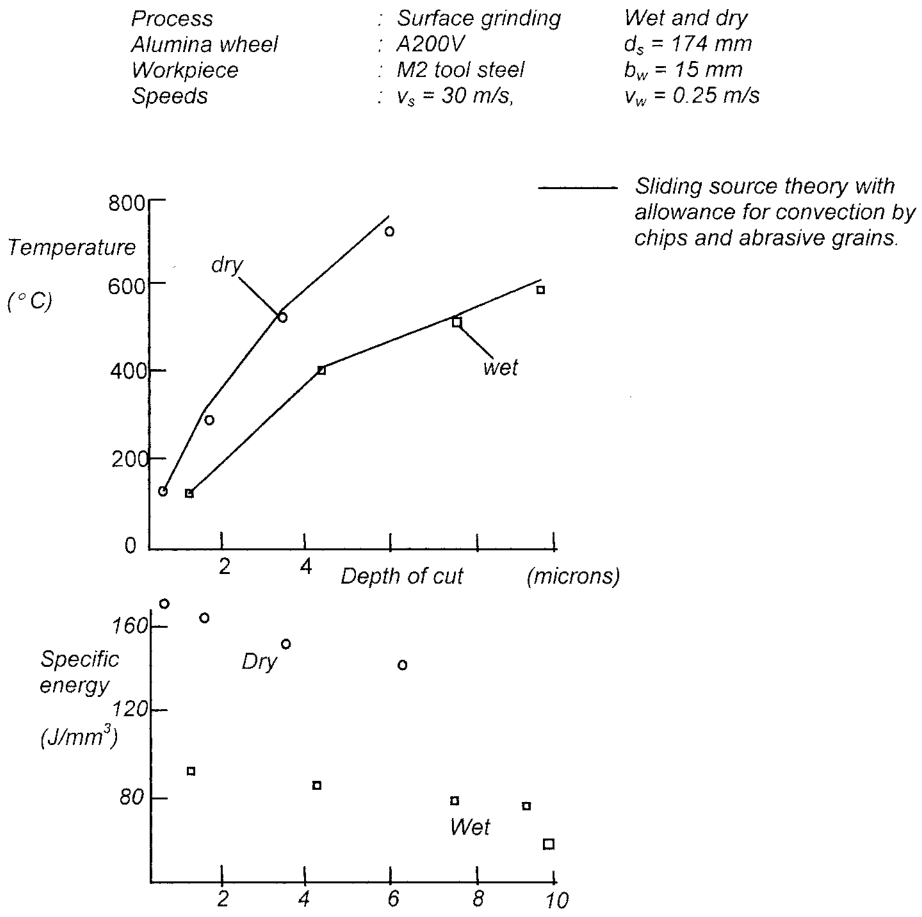

Fig. 5 In shallow cut grinding the main effect of the grinding fluid is to reduce the specific energy and hence the temperatures

For a more complete understanding of the effect of any process variable, it is necessary to examine more closely the heat transfer in the region of the abrasive contact.

5 HEAT CONDUCTION WITHIN THE WORKPIECE

The heat flux, q_w, conducted into the workpiece is only a proportion of the total heat flux, q_t. Defining this proportion as R_w, the heat flux which enters the workpiece is

$$q_w = R_w q_t \tag{3}$$

Table 3 Typical values of depth of cut, contact length and contact time in shallow grinding and creep grinding

	Creep grinding	Shallow grinding
Depth of cut	7 mm	0.04 mm
Wheel diameter	200 mm	200 mm
Work speed	0.005 m/s	0.2 m/s
Contact length	37.4 mm	2.8 mm
Contact time	7.48 s	0.014 s

Since q_t varies as a function of position in the contact zone as in equation (2), this expression can be written more generally as

$$q_w(x) = R_w q_t(x) \tag{4}$$

The value of R_w is not actually a constant throughout the contact zone but this assumption is made for simplicity. Typically, the average workpiece partition ratio, R_w, varies according to the type of abrasive, the workpiece material, the specific energy, the grinding fluid and the contact length. For grinding with an alumina wheel in a dry shallow cut operation, the value of R_w may be as high as 90 per cent, whereas in well-lubricated creep grinding the partition ratio may be less than 5 per cent.

Further work is required to determine how values of R_w are affected by inclining the heat source at an angle. However, the effect of the inclination will always reduce workpiece temperatures on the finished workpiece surface even if R_w is increased. The determination of R_w will be discussed later after considering how heat conducts into a workpiece.

First an analysis is needed for the heat conduction into the workpiece. In order to achieve a solution, a simplifying assumption is made that the heat source lies within a semi-infinite plane. This assumption has always been implicit in sliding source solutions where the heat source is assumed to lie in the plane of the finished workpiece and is also assumed to lie in the same plane as the uncut workpiece surface. This is clearly untrue, since the heat source lies on a curved inclined surface. However, it can be shown that, if the inclination of the surface containing the heat source is small and the Peclet number is large, the errors will be negligible. For deep cuts the prime area of interest lies immediately at and under the heat source. For large angles of inclination, it is clearly more appropriate to estimate the temperatures in this region by modelling the heat source as a moving inclined heat source rather than as a sliding heat source. In a further paper to be published, the modification of the temperature profile due to deviations of the workpiece surface from a flat plane is estimated. Further modifications will be introduced into the model to account for the curved contact surface and also for the change in the boundary conditions outside the contact zone. However, the modifications resulting from the 'non-planar' surface introduce a level of complexity into the analysis and results which go beyond the extent of this paper.

The following general approach can be used to obtain a temperature solution for any shape of heat flux distribution across the contact length for the inclined or sliding heat source within a semi-infinite plane.

The band of heat in a practical grinding contact is usually considered as a series of moving line source elements. The temperatures which result from a moving line source can be obtained using Bessel functions which are available from tables or as functions in mathematical software. The temperatures resulting from a continuous band of line sources must be summed over the length of the grinding contact. This summation process is expressed by the integrals in equation (5) assuming a semi-infinite workpiece.

The band heat source is considered to lie in the inclined plane defined by equation (6). The solution for an inclined band source moving in the x direction with flux q varying in strength with position a within the contact length is given by

$$T = \int_{-l_c/2}^{+l_c/2} \frac{q}{\pi k} e^{v(x - a\cos\phi)/2\alpha} K_0 \times \left\{ \frac{v[(x - a\cos\phi)^2 + (z - a\sin\phi)^2]^{1/2}}{2\alpha} \right\} da \quad (5)$$

where $K_0(u)$ is the modified Bessel function of the second kind of order zero for an argument of value u. The parameter q should be interpreted as q_w, the heat which enters the workpiece, and v should be interpreted as v_w, the work speed. All parameters are to be specified with respect to the workpiece material.

The integration variable a may be defined for various positions of the line source elements within the heat band

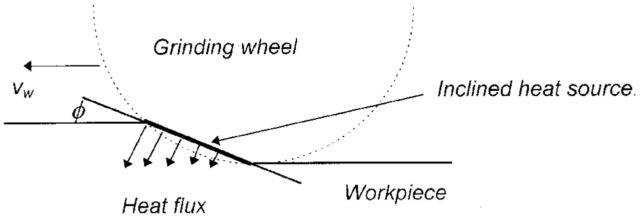

Fig. 6 The inclined heat source. The contact zone is represented by the straight line at an angle ϕ to the direction of movement

according to the relations in the following equation and Fig. 7:

$$-\frac{l_c}{2} \leqslant a \leqslant \frac{l_c}{2}, \qquad \text{where } x = a\cos\phi \text{ and } z = a\sin\phi \quad (6)$$

The contact zone as illustrated in Fig. 6 is represented by a straight incline. Solutions for a curved contact zone give slightly different results but, since the curvature of the two surfaces in contact is always very large in relation to the depth of the thermally affected layer, the errors in the estimation of the maximum temperature due to curvature are small compared with the effect of the inclination angle. A more significant error arises because the angle of inclination varies throughout the contact length. An extensive analysis of the errors will be presented in a future paper in the course of preparation.

The thermal properties of the workpiece material are represented by k, ρ, c and α where

k is the mean thermal conductivity
ρ is the density
c is the mean specific heat capacity

and

$$\alpha = \frac{k}{\rho c}$$

is the mean diffusivity.

Surface temperatures calculated from equation (5) are given in Fig. 7 for a triangular heat distribution. In the figure, it appears that the band source width decreases with angle of inclination. This is because the length of the band source projected onto the x–y plane decreases with inclination. Temperatures to the left and right of the ends of the band source are shown but are not accurate owing to the discontinuities in the geometry of the real workpiece at the two ends. These lower temperatures outside the contact region are of little interest. Of more significance, it is found that, at very low Peclet numbers, an error is introduced into the estimate of the maximum temperature within the contact zone. For high values of the Peclet number, the error is negligible. For very low values of the Peclet number, the temperature trends indicated are of a similar nature in spite of

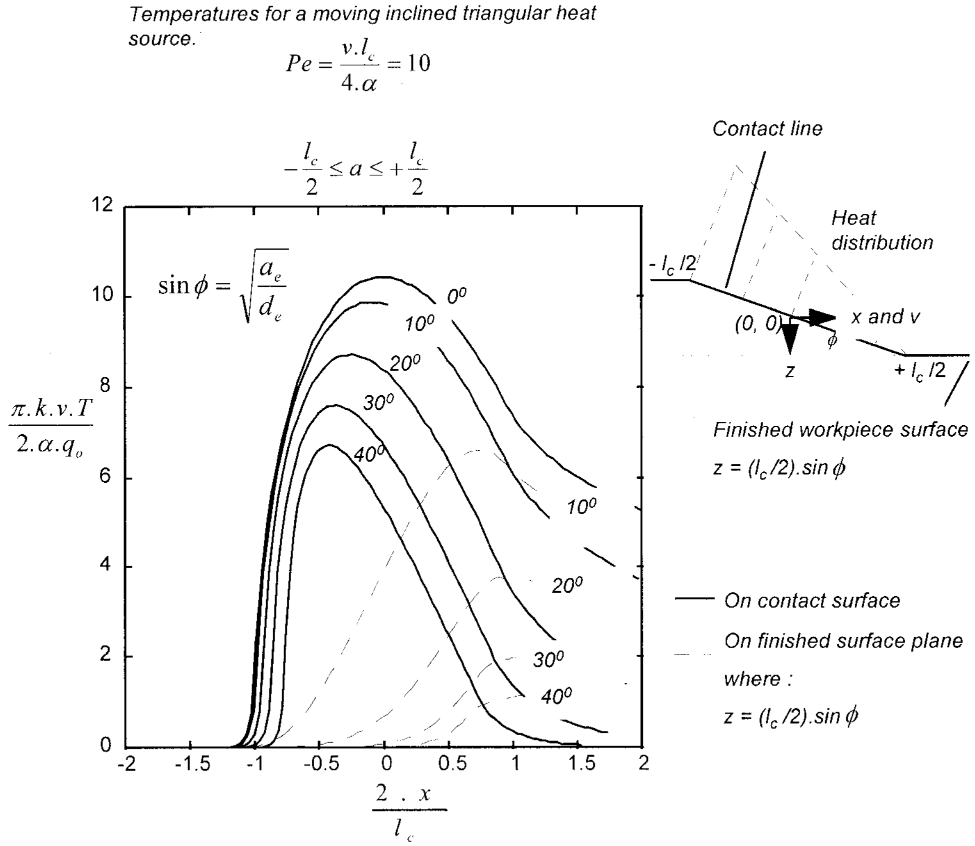

Fig. 7 Contact surface temperatures (full curves) and temperatures in the plane of the finished workpiece (broken curves) for an inclined heat source with a triangular distribution. $Pe = 10$

the error. Under these conditions there is an increase in the maximum temperature due to the 'missing' material ahead of the contact compared with the assumption of a true semi-infinite plane.

For very deep cuts, the resulting temperatures are much lower than found by modelling the heat as a distribution sliding in the direction of motion. Setting the inclination angle to zero gives the usual results for a sliding source. It is therefore seen that it is more accurate to model the heat source as distributed along the contact length represented as an inclined plane or as an arc. Not only are the temperatures along the contact surface reduced with angle of inclination but, even more impressively, the temperatures in the plane of the finished surface are greatly reduced. For example, with an angle of inclination $\phi = 30°$, the maximum temperature on the finished surface is less than one-fifth of the value for $\phi = 0°$.

On the plane of the finished workpiece surface the maximum temperature is close to the end of the contact length where the wheel leaves contact with a position on the workpiece. However, if the temperatures along the contact arc are examined, the maximum temperature moves towards the start of contact with increasing angle. This is because the temperatures correspond more closely to the shape of the flux distribution with increasing angle.

For the triangular flux, the maximum temperature occurs at the midpoint of the band at high values of the Peclet number Pe, typical of grinding. This is different from the case of a uniform heat flux where the maximum temperature occurs at the trailing edge of the contact zone. This point has significance for deep grinding since the temperatures on the finished workpiece surface are further reduced with the triangular assumption. The triangular assumption is also important for the correct interpretation of measured temperature signals.

The effect of Peclet number on temperatures for a sliding heat source is shown in Fig. 8. The Peclet number is a dimensionless parameter proportional to the speed of the heat source. It is also proportional to the contact length of the sliding heat source and inversely proportional to the thermal diffusivity of the material under the heat source. For the background workpiece temperature, the relevant sliding speed is the workspeed v_w:

$$Pe = \frac{v_w l_c}{4\alpha} \tag{8}$$

where l_c is the width of the heat source, v_w is the sliding speed and α is the thermal diffusivity as defined by equation (7). In Fig. 7, the motion and the contact length no longer lie in the same plane, so the equivalent

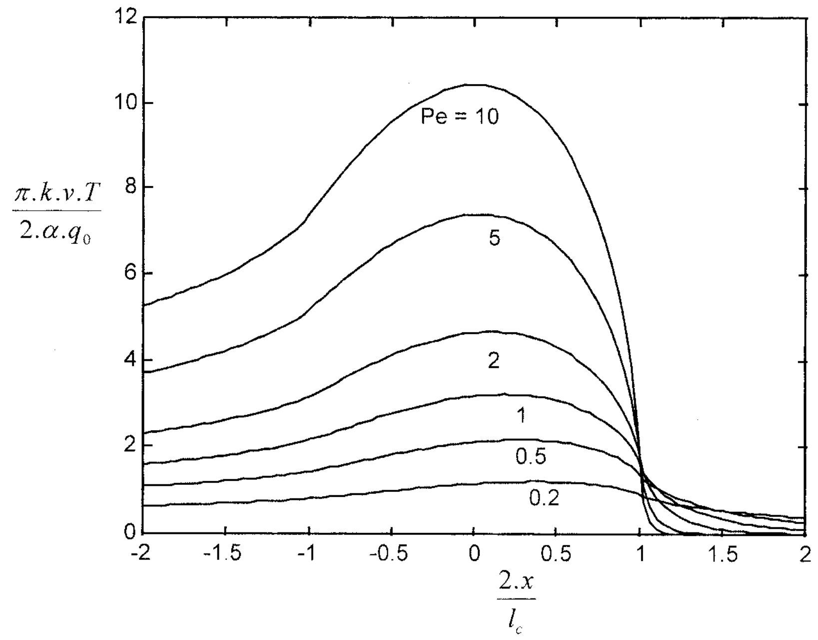

Fig. 8 Contact surface temperatures for different values of the Peclet number with a triangular heat source. The heat source in this case is sliding from left to right at a speed v with $\phi = 0$

value of the Peclet number is expressed in the same way as Pe in equation (8).

In most cases, grinding conditions correspond to a high value of the Peclet number. For a typical cast iron,

$$v_w = 0.2\,\text{m/s}$$

$$l_c = 0.002\,\text{m}$$

$$\alpha = 14.4 \times 10^{-6}\,\text{m}^2/\text{s}$$

$$Pe = \frac{0.2 \times 0.002 \times 10^{-6}}{4 \times 14.4} = 6.94$$

Table 4 Approximate thermal properties of typical engineering materials

	Conductivity (W/m K)	Density (kg/m^3)	Specific heat (J/kg K)	$\beta = \sqrt{k\rho c}$ (J/m^2 s K)
Cast iron (260)	53.7	7300	511	14 150
AISI 1055	42.6	7840	477	12 620
M2	23.5	7860	515	9 750
AISI 52100	34.3	7815	506	11 650

Table 5 Approximate thermal properties of typical abrasive grains

	Conductivity (W/m K)	Density (kg/m^3)	Specific heat (J/kg K)	$\beta = \sqrt{k\rho c}$ (J/m^2 s K)
Diamond	2000	3520	511	60 000
CB Nitride	240 (pure—up to 1300)	3480	506	20 600 (48 000)
Silicon carbide	100	3210	710	15 100
Aluminium oxide	35	3980	765	10 300

Some typical values of thermal properties for common engineering materials are given in Table 4. Values for abrasive grains are given in Table 5.

6 APPROXIMATE SOLUTIONS FOR MAXIMUM TEMPERATURE

Temperatures may be read from charts such as Figs 7 and 8 or calculated from equation (5). For shallow cut processes using alumina or silicon carbide abrasives, a crude approximation can be made that all the energy enters the workpiece (that is, $R_w = 1$). This assumption overestimates the temperatures usually by at least 25 per cent. The overestimate is even greater with low values of specific energy because the chip energy becomes more significant. For CBN, the conduction into the grains is much greater and the crude approximation is too inaccurate. Methods of energy partitioning are discussed below. For the time being, it is simply assumed that the energy entering the workpiece can be determined.

In some situations it is required to calculate the temperatures throughout the contact zone. An example arises in creep grinding where the long arc of contact gives rise to strong fluid convection from the workpiece surface. Convection of heat is proportional to temperature, so that it is necessary to evaluate temperatures throughout the region to determine the magnitude of the convection to the fluid

At high sliding speed ($Pe > 5$), surface temperatures in shallow grinding may be estimated from the equation for a moving plane heat source. For the sliding triangular source, an approximate solution can be obtained by integrating the temperature solution for an instantaneous line source with varying flux strength. The line source solution is

$$T = \frac{q_0}{\sqrt{\pi (k\rho c)_w}} t^{-1/2} e^{-z^2/4\alpha t} \tag{9}$$

The flux can be expressed as a function of time from start $t = 0$ to the end of the arc of cut $t = t_c$:

$$q = 2q_0(1 - t/t_c) \tag{10}$$

The moving band temperatures are then given by

$$T = \int_0^t \frac{2q_0}{\sqrt{\pi k\rho c}} t^{-1/2} \left(1 - \frac{t}{t_c}\right) e^{-z^2/4\alpha t}\, dt \tag{11}$$

Evaluation of the integral at the surface gives

$$T = \frac{4q_0}{\sqrt{\pi k\rho c}} t^{1/2} \left(1 - \frac{2t}{3t_c}\right) \tag{12}$$

The maximum temperature is given when $t = 0.5t_c$ from which it is found that

$$\frac{T\pi k v}{2\alpha q_0} = 3.34\, Pe^{1/2} \qquad (Pe > 10) \tag{13}$$

For a uniform heat flux the factor in equation (13) is 3.54 whereas for the triangular flux the factor is 3.34. The approximation is seen to work very well for high values of the Peclet number and it works with reasonable accuracy across a range of values. The expressions for the maximum temperatures can be expressed in many different forms. One of the simplest forms for abrasive machining contacts is

$$T = C R_w \frac{q_t}{\beta} \sqrt{\frac{l_c}{v_w}} \tag{14}$$

where $\beta = \sqrt{(k\rho c)_w}$ is the thermal property of the workpiece material, l_c is the contact length, v_w is the work speed, q_t is the heat flowrate (or power) per unit area and R_w is the proportion of the heat which enters the workpiece. In equation (13), it is necessary to replace q_0 by $R_w q_t$ to allow for the fact that only a proportion R_w of the total heat generated is conducted into the workpiece. C is a constant which from equation (13) is approximately equal to 1. More accurate values can be determined by integrating equation (5) or from the values given in Figs 7 and 8.

If l_g is used instead of l_c for the contact length an error is introduced in shallow grinding. For a grinding condition where the contact length $l_c \approx 2l_g$, it is found that using l_g instead of l_c predicts a temperature which is overestimated by 41 per cent. This can be shown by writing equation (14) in terms of power:

$$T = C \frac{R_w P}{\beta b_c l_c} \sqrt{\frac{l_c}{v_w}} \tag{15}$$

On substituting $0.5l_c$ for l_c, it is seen that the result is proportional to the square root of l_c and the error is $1.41 - 1 = 41$ per cent.

7 HEAT FLOWS IN THE CONTACT AREA AND PARTITIONING

The total heat in the contact area flows out along four paths as in Fig. 9. For convenience the total machining power is represented as a heat flux according to equation (1). The four heat flows are, therefore,

$$q_t = q_w + q_s + q_{ch} + q_f \tag{16}$$

The proportions of the heat to the total must be equal to unity:

$$1 = R_w + R_s + R_{ch} + R_f \tag{17}$$

where $R_w = q_w/q_t$ and so on.

R_w is the workpiece partition ratio as required in equation (15) to calculate the maximum workpiece temperature. R_w can also be determined from measurements of maximum temperature using equation (15). This allows measurements to be compared with predictions so that thermal models can be refined to achieve agreement over a wide range of operating conditions. R_w can be calculated theoretically, which requires the prediction of values of R_s, R_{ch} and R_f.

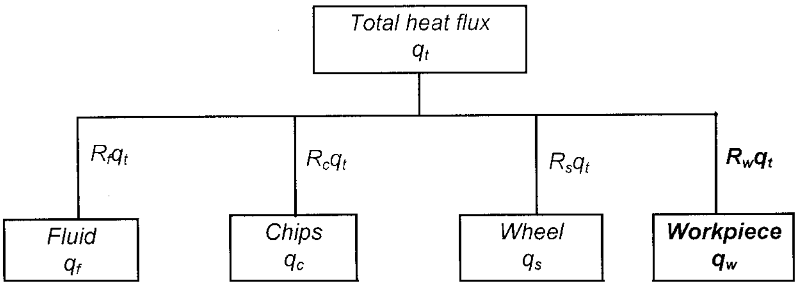

Fig. 9 Partitioning of the heat generated in the contact area to the fluid, the chips, the abrasive and the workpiece

7.1 Heat flow to the chips

Assuming that the chips reach a temperature close to but not greater than the melting temperature as previously discussed, the heat flux to the chips is

$$q_{\mathrm{ch}} = \rho c T_{\mathrm{mp}} \left(\frac{a_{\mathrm{e}} v_{\mathrm{w}}}{l_{\mathrm{c}}} \right) \tag{18}$$

where

ρ = density of the workpiece material

c = specific heat capacity

T_{mp} = melting temperature

a_{e} = real depth of cut

v_{w} = work speed

l_{c} = contact length

7.2 Heat flow to the process fluid

The heat flow to the process fluid depends on whether the contact zone temperatures remain below the boiling temperature or whether this temperature is substantially exceeded. Where fluid boiling is avoided, the heat convected by the fluid is proportional to the average surface temperature T_{av}, the contact area bl_{c} and the convection coefficient h_{f}. The heat flowrate to the fluid per unit area of the contact surface is the flux q_{f} and is therefore

$$q_{\mathrm{f}} = h_{\mathrm{f}} T_{\mathrm{av}} \tag{19}$$

In general, the average temperature in the contact area is approximately two-thirds the maximum temperature, so that for non-boiling situations

$$q_{\mathrm{f}} = \tfrac{2}{3} h_{\mathrm{f}} T_{\max} \tag{20}$$

It is usually more convenient to compute the maximum temperature and this can be used as a measure of the average temperature for the purpose of estimating the fluid convection effect.

In many cases, fluid boiling temperatures are exceeded. In shallow cut grinding, convection plays a relatively small role in heat dissipation within the contact area, so that it is less important if the fluid boils. In deep grinding, fluid convection predominates so boiling is more significant. If the boiling temperature is only just reached, there may still be substantial cooling due to convection in part of the contact area and also evaporative cooling with nucleate boiling. However, if the boiling temperature is substantially exceeded in creep grinding, a numerical solution might be expected to allow a more accurate estimate of temperatures taking convection into account.

The supply of fluid in sufficient volume is important even if boiling temperatures are exceeded not only for cooling but also for lubrication and to minimize wheel loading.

7.3 Heat sharing between the workpiece and the abrasive grains

The heat flow q_{ws} shared by the workpiece and the abrasive given by rearrangement of equation (16) is

$$q_{\mathrm{ws}} = q_{\mathrm{w}} + q_{\mathrm{s}} = q_{\mathrm{t}} - q_{\mathrm{ch}} - q_{\mathrm{f}} \tag{21}$$

The problem is to distinguish the proportions of q_{ws} shared by the abrasive grains and by the workpiece. There are several methods of partitioning the heat flow between the abrasive and the workpiece. This problem may be resolved using the Hahn model [**3**, **21**]. Approximate values quoted in the case studies which follow are readily available for either conventional or CBN abrasives. These models provide a workpiece–abrasive partition ratio R_{ws} where

$$R_{\mathrm{ws}} = \frac{q_{\mathrm{w}}}{q_{\mathrm{w}} + q_{\mathrm{s}}} = \left[1 + \frac{k_{\mathrm{ge}}}{\sqrt{r_0 v_{\mathrm{s}} (k\rho c)_{\mathrm{w}}}} \right]^{-1} \tag{22}$$

R_{ws} remains reasonably constant for a particular workpiece–abrasive combination. The value may be calculated from equation (22) using the thermal properties of the abrasive grain and the workpiece material. An average value of the effective contact radius of the grain is 20 μm.

7.4 Heat flow to the workpiece

From equations (21) and (22) the heat flow to the workpiece is

$$q_{\mathrm{w}} = R_{\mathrm{ws}} (q_{\mathrm{t}} - q_{\mathrm{ch}} - q_{\mathrm{f}}) \tag{23}$$

7.5 Maximum workpiece temperature

From equation (23), the maximum workpiece temperature can be expressed in terms of R_{ws} which is assumed to remain constant for a particular wheel and workpiece combination:

$$T_{\max} = R_{\mathrm{ws}} (q_{\mathrm{t}} - q_{\mathrm{ch}} - q_{\mathrm{f}}) \frac{C}{\beta} \sqrt{\frac{l_{\mathrm{c}}}{v_{\mathrm{w}}}} \tag{24}$$

For the non-boiling case, it is possible to substitute for q_{c} and q_{f} from equations (18) and (20) so that, at last, a solution is obtained for the maximum temperature in the contact region:

$$T_{\max} = \frac{q_{\mathrm{t}} - \rho c T_{\mathrm{mp}} a_{\mathrm{e}} v_{\mathrm{w}} / l_{\mathrm{c}}}{[\beta / (R_{\mathrm{ws}} C)] \sqrt{v_{\mathrm{w}} / l_{\mathrm{c}}} + \frac{2}{3} h_{\mathrm{f}}} \tag{25}$$

With suitable, even approximate, values of R_{ws} equation (25) can be used to estimate maximum temperature in an abrasive contact zone. Equation (25) can be written in concise form as

$$T_{\max} = \frac{3}{2} \frac{q_t - q_c}{h_w/R_{ws} + h_f} \tag{26}$$

where

$$h_w = \frac{3}{2} \frac{\beta}{C} \sqrt{\frac{v_w}{l_c}} \tag{27}$$

Equation (25) may be used to examine the importance of the various convection factors in particular examples of grinding processes.

8 CASE STUDIES

8.1 Case study 1: shallow cut grinding—10 μm cut

The maximum temperature in the contact zone is to be estimated for the grinding conditions in Table 6.

The Peclet number is found to be greater than 10. In shallow grinding, by reference to equations (13) and (14) it is therefore found that the value $C = 1.07$ can be used in equation (25) for a sliding heat source:

$$Pe = \frac{v_w l_c}{4\alpha} = 25.9$$

The removal rate per unit width of cut (specific removal rate) is given by

$$Q'_w = a_e v_w = 3\,\text{mm}^2/\text{s}$$

The total heat flux can be determined from the specific energy and the removal rate:

$$q_t = \frac{e_c Q_w}{b_w l_c} = \frac{e_c Q'_w}{l_c} = 40\,\text{W/mm}^2$$

The maximum energy to the chips, $e_{ch} = 6\,\text{J/mm}^3$, may be represented as a heat flux since

$$q_{ch} = \frac{e_{ch} Q_w}{b_w l_c} = \frac{e_{ch} Q'_w}{l_c} = 6\,\text{W/mm}^2$$

Table 6 Grinding conditions for case study 1

d_e	200 mm	Equivalent diameter
e_c	40 J/mm^3	Process specific energy
e_{ch}	6 J/mm^3	Specific energy to chips
v_s	30 m/s	Wheel speed
v_w	0.3 m/s	Work speed
a_e	10 μm	Depth of cut
l_c	3 mm	Contact length
k_w	34.3 W/m K	Workpiece conductivity
ρ_w	7810 kg/m^3	Workpiece density
c_w	506 J/kg K	Workpiece specific heat
R_{ws}	0.8	Work–wheel partition ratio
b_w	15 mm	Contact width
h_f	10 000 W/m^2 K^1	Convection coefficient for fluid

The thermal property of the workpiece material is given by

$$\beta = \sqrt{k_w \rho_w c_w} = 11\,640\,\text{J/m}^2\,\text{K}\,\text{s}^{0.5}$$

The coefficient for conduction into the workpiece is given by

$$h_w = \frac{3}{2} \frac{\beta}{C} \sqrt{\frac{v_w}{l_c}} = 163\,200\,\text{W/m}^2\,\text{K}$$

The maximum temperature is therefore estimated as

$$T_{\max} = \frac{3}{2} \frac{q_t - q_{ch}}{h_w/R_{ws} + h_f} = 238\,^\circ\text{C}$$

A temperature of 238 °C means that the workpiece is below the tempering and oxidation region. With water-based coolants, fluid boiling will be experienced but this is unlikely to be a problem in shallow cut grinding. At higher temperatures where thermal damage is a problem, action should be taken to reduce the specific energy. This may be achieved by one of several methods such as re-dressing the wheel, using a coarser dressing feed, using a more open or softer wheel and improving the coolant supply for more effective lubrication. Problems experienced may also be overcome by reducing the depth of cut to reduce the total heat flux or even reducing the wheel speed to increase the uncut chip thickness.

If the calculation had been carried out ignoring heat flows to the chips, the fluid and wheel, the calculation is simplified but the maximum temperature is overestimated by 54 per cent:

$$T_{\max} = \frac{3}{2} \frac{q_t}{h_w} = 368\,^\circ\text{C}$$

compared with the more accurate result of 238 °C.

Using the geometric contact length instead of the real contact length increases the temperature to approximately 218 per cent of the more accurate value. Taking the chip energy into account, in this example, reduced the temperature predicted by 15 per cent. Taking fluid convection into account reduced the predicted temperature by approximately 5 per cent. Of course, in this example, water-based fluid would have boiled and part of the cooling would have come from evaporative cooling rather than conventional convective cooling.

8.2 Case study 2: creep grinding—1 mm cut

The conditions are the same as in the previous case except that the depth of cut is increased and the work speed is reduced to maintain the same removal rate (see Table 7).

The new results which may be compared with the previous results using the sliding source model are as follows:

Table 7 Changed conditions for case study 2

a_e	1 mm	Depth of cut
l_c	14 mm	Contact length
v_w	0.003 m/s	Workspeed

$$Pe = 1.21$$

$$C = 0.79$$

$$Q'_w = 3\,\text{mm}^2/\text{s}$$

$$q_t = 8.57\,\text{W/mm}^2$$

$$q_{ch} = 1.28\,\text{W/mm}^2$$

$$q_t - q_{ch} = 7.29\,\text{W/mm}^2$$

$$h_w = 0.0102\,\text{W/mm}^2\,\text{K}$$

$$h_f = 0.01\,\text{W/mm}^2\,\text{K}$$

$$T_{max} = \frac{1.5 \times 7.29}{0.0102/0.8 + 0.01} = 480\,^{\circ}\text{C}$$

Although the removal rate is unchanged, the heat flux is reduced to 21 per cent of its previous value. This is entirely due to the change in the contact length which benefits fluid convection.

The factor h_w for conduction into the workpiece is reduced by 16 times owng to the reduced workspeed and the increased contact length. As a result of the reduction in h_w, the conduction into the workpiece is only slightly larger than the convection to the fluid, since h_f is only slightly smaller than h_w.

The resultant temperature is more than doubled, which appears to suggest that reducing work speed is a bad idea. Also, since the maximum temperature is well above the boiling temperature of a process fluid, it must be assumed that 'burn-out' will occur and the maximum temperature will be even higher. The grinding conditions should therefore be changed if possible to reduce the temperatures to below the fluid 'burn-out' temperature.

If it is assumed that because of boiling the fluid is effective up to 140 °C, the heat extracted by the fluid is reduced to 40 per cent of its previous value. Adopting an approximate factor of $140/(480 \times 2/3)$ for the convection coefficient, the temperature can be estimated for $h_f = 4000\,\text{W/m}^2\,\text{K}$. This yields

$$T_{max} = 643\,^{\circ}\text{C}$$

In practice, it might be envisaged that a hot spot will grow from the region of the maximum temperature because convection cooling no longer applies uniformly across the contact, leading to an even higher peak temperature. It can also be visualized, depending on the direction of wheel rotation, that one side or the other will be starved of coolant once boiling has occurred. This will further extend the hot region.

Since the operation is creep grinding, the effect of the inclined heat source assumption as expressed by equation (5) should be considered. The contact angle is given by

$$\sin\phi = \sqrt{\frac{a_e}{d_e}}$$

For this case, the angle $\phi = 4°$. Referring to Fig. 7, it is seen that the maximum temperature on the contact surface is reduced by less than 5 per cent. The maximum temperature experienced by the finished workpiece surface is further reduced by approximately 10 per cent. Before concluding that the inclined heat source has an insignificant effect it should be appreciated that the depth of cut in this example is small by the standards of creep grinding and HEDG. Further examples will demonstrate this point.

The maximum temperatures predicted taking fluid convection into account suggest that the surface will be damaged even taking the benefits of the inclined heat source into account. For such high temperatures, special measures need to be taken, such as high pressure wheel cleaning and oil lubrication to prevent wheel loading and serious loss of grinding efficiency. If at all possible, such high temperatures will be avoided. Where dry conditions apply, Lee *et al.* [**22**] proposed that $h_f = 500\,\text{W/m}^2\,\text{K}$ approximately.

8.3 Case study 3: creep grinding—20 mm cut

The high temperatures in the previous case are to be overcome by further increasing the depth of cut to 20 mm and reducing the work speed to 0.015 mm/s, maintaining the specific removal rate at 3 mm^2/s (see Table 8).

The maximum temperature is reduced to

$$T_{max} = \frac{1.5 \times 1.62}{0.0011/0.8 + 0.01} = 213\,^{\circ}\text{C}$$

Whereas in case study 2 the move to creep feed grinding increased temperature, the further increase in depth of cut and reduction in work speed reduce temperature. The reduction in temperature is due to the increased contact length.

Table 8 Changed conditions for case study 3

a_e	20 mm	Depth of cut
v_w	0.000 15 m/s	Work speed
Accordingly:		
l_c	63.2 mm	Contact length
q_t	1.9 W/mm^2	Total flux
q_{ch}	0.28 W/mm^2	Flux convected by chips
$q_t - q_{ch}$	1.62 W/mm^2	
h_w	0.001 12 W/mm^2 K	Factor for workpiece conduction
h_f	0.01 W/mm^2 K	Fluid convection factor

The predicted temperature is still above the boiling temperature for a water-based fluid and therefore the calculation which assumed $h_f = 10\,000\,\mathrm{W/m^2\,K}$ suggests that the predicted temperature is likely to be an underestimate. On this basis, a further increase in depth of cut and reduction in work speed appear to be required to bring the temperature down and to ensure a completely satisfactory process.

If the angle of inclination is now taken into account according to equation (5), it is found that the maximum temperature is reduced. First, on calculating the angle of inclination using the expression given in the previous example, it is found that $\phi = 17.5°$. On referring to Fig. 7, the maximum temperature appears to be reduced by approximately 20 per cent for this inclination. This reduction in temperature is equivalent to increasing the factor for conduction into the workpiece by 25 per cent. Increasing h_w by 25 per cent decreases the maximum temperature to 207 °C which is a rather small reduction. The reduction in temperature is small owing to the predominance of fluid convection over workpiece conduction. The effect of the angle of inclination on temperature is much more substantial in dry grinding which will be seen when HEDG is considered. A further factor which offsets the advantages of the inclined plane source solution in this example is the very low Peclet number. In this example, $Pe = 0.027$. For such a low value of the Peclet number, the values given in Fig. 7 are no longer accurate. Equation (5) needs to be recomputed for the low value of the Peclet number and account taken of the non-planar heat source

It can also be seen from Fig. 7 that the maximum temperature experienced by the finished workpiece surface with this angle of inclination is more than halved. While the contact surface experiences a modest reduction in maximum temperature, the finished surface experiences a substantial reduction in temperature.

Figure 10 illustrates the effect of increasing depth of cut at a reduced removal rate, $Q'_w = 1\,\mathrm{mm^2/s}$, based on the sliding source model. The process can now be carried out with cool grinding, either at depths of cut smaller than 0.005 mm or at depths of cut larger than 8 mm, as long as there is a plentiful supply of fluid to achieve the value $h_f = 10\,000\,\mathrm{W/m^2\,K}$.

In conventional grinding, successful grinding can be achieved at temperatures above boiling. Below the peak values in the mid-range, shown in Fig. 10, workpiece conduction predominates over fluid convection. The loss of convection is therefore less important as a determinant of maximum temperature in shallow grinding. In creep grinding, with depths of cut greater than 0.2 mm convection is increasingly important to achieve effective cooling. However, at a depth of cut of 8 mm, it is possible to achieve very cool grinding, at $T_{max} = 110\,°\mathrm{C}$.

Since convection predominates, the maximum temperature will occur between the entry where the maximum energy is generated and the midpoint of the contact region. This is also the expectation from Fig. 7. Because of the large angle of inclination, the maximum temperature experienced by the finished workpiece surface will be even lower than this value.

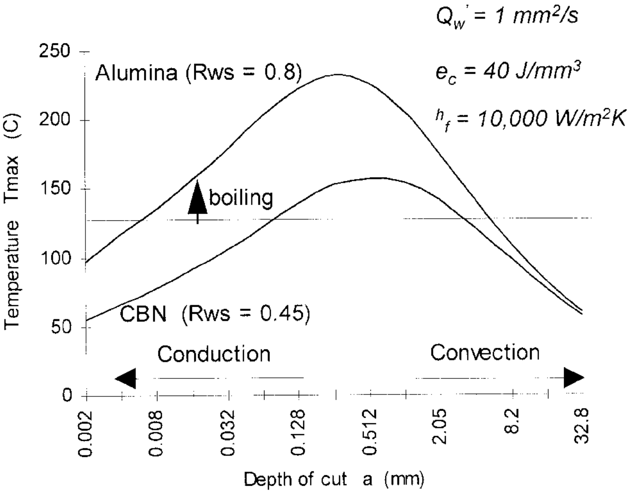

Fig. 10 Maximum contact surface temperatures in conventional and creep-feed grinding using alumina and CBN wheels based on the sliding source model. No allowance has been made for fluid boiling. The boiling temperature shown is an approximate value for oil in water emulsion

The temperature model demonstrates similar values to the results presented by Werner [**23**], who found there was an intermediate range of depths of cut where thermal damage was likely.

CBN abrasives reduce temperature substantially as shown in Fig. 10. The reduction is due to the high thermal conductivity of CBN. The value of the thermal conductivity is reflected in the value of R_{ws}.

Specific energy is an inverse measure of the cutting efficiency of the grinding wheel and workpiece material combination for the particular process conditions. Figure 11 is a chart of predicted temperatures using the sliding source model for various values of specific energy at a constant specific removal rate $Q'_w = 1\,\mathrm{mm^2/s}$, using an alumina wheel to machine AISI 52100.

8.4 Case study 4: high efficiency deep grinding

A development in recent years combines the advantages of deep grinding as demonstrated in the previous examples with the advantages of high work speeds as employed in conventional grinding. Combining these two factors minimizes the heat conducted into the workpiece. High wheel speeds, 80–200 m/s, are also employed to minimize the grinding forces and reduce the rate of wheel wear.

The concept of HEDG was first proposed by Guhring [**24**]. The principles were largely developed by Werner

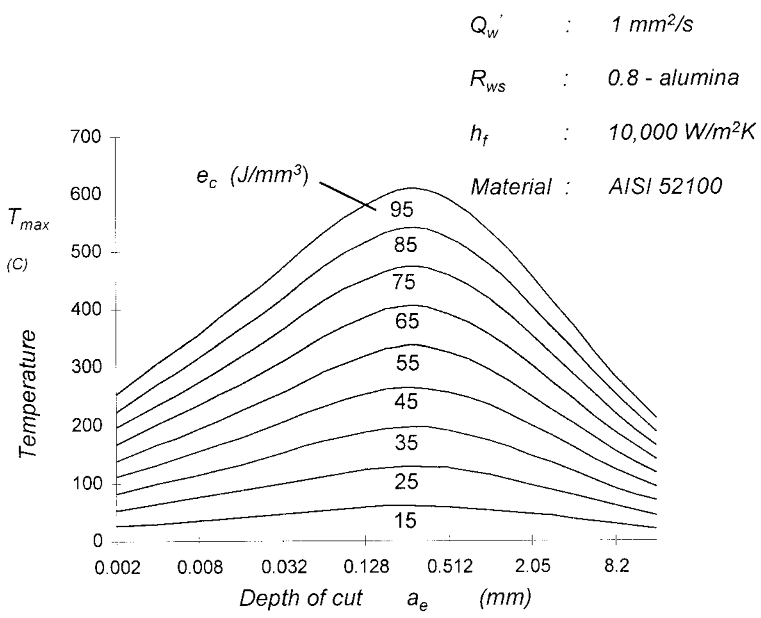

Fig. 11 Effect of specific energy on maximum temperature based on the sliding source model

and further described by Tawakoli [23]. To achieve HEDG requires large depths of cut as in creep grinding, combined with a large power supply and drive motor to cope with the extremely high removal rates.

Above all, the process requires very low specific energy values to be achieved to limit temperature rise. It therefore helps if the materials machined at high wheel speeds are of the type known as 'easy to grind'. These include free machining cast irons and steels. Difficult-to-grind materials must be machined at lower wheel speeds. The use of CBN abrasives also helps to reduce temperature rise. CBN wheels of the electroplated or metal-bonded type are mainly used to withstand the bursting stresses at the high speeds involved and for chemical stability at high temperatures. High speed silicon carbide wheels may also be used but at rather lower speeds. Care must be taken to ensure appropriate guarding in case of a wheel burst.

The requirements for successful grinding are even more critical in HEDG than in other abrasive processes. In particular, several coolant nozzles may be required to ensure that high velocity fluid penetrates the boundary layer around the wheel and is absorbed into the pores of the wheel. Sometimes a pressurized shoe is fitted around a portion of the circumference and the sides of the wheel to ensure fluid penetration. In addition, high pressure jets are employed to clean away swarf from the wheel surface. This is because wheel loading quickly destroys the cutting efficiency of the wheel. Other aspects of machine design for HEDG are described by Tawakoli [23].

The principle of HEDG is very interesting since a new physical principle is involved. Previously, it was argued that the chip temperature could not exceed the melting temperature of the material. This limits the energy which can be absorbed by the chips. Now an additional physical limitation is introduced to the analysis, that the background temperature of the workpiece contact surface cannot exceed the melting temperature of the material. According to equations (15) and (25), the melting temperature limitation places a limitation on the energy generated by the process.

This principle is illustrated in Fig. 12 using the sliding source model for depths of cut at relatively small angles of inclination. Convection is ignored in the computation to illustrate the effect of melting temperatures on the contact surface in dry grinding. Even with very low values of specific energy, melting temperature is quickly achieved if convection is ignored. This corresponds roughly to the situation where burn-out of the process fluid occurs. The case for a specific energy of 40 J/mm^3 is particularly interesting. A ceiling of 1500 °C has been imposed in the computation for the maximum contact temperature. It can be seen that as depth of cut is further increased the temperature line converges with the line for a specific energy of 11 J/mm^3 and with further increases in depth of cut will converge with the line for a specific energy of 7 J/mm^3. Tawakoli quotes one example of a specific energy of 7.05 J/mm^3. This must be close to the minimum ultimately achievable for steels, since it is close to the melting energy of the material.

On the basis purely of the principles of heat transfer, it becomes apparent that the physical limitation of the melting temperature also represents a limitation on the heat generated in the contact zone. The precise values of the heat flows are debatable but the overwhelming conclusion points in this direction. In other words, low specific energy can be achieved if the background temperature of the contact surface is allowed to approach the melting temperature so that shear forces are greatly

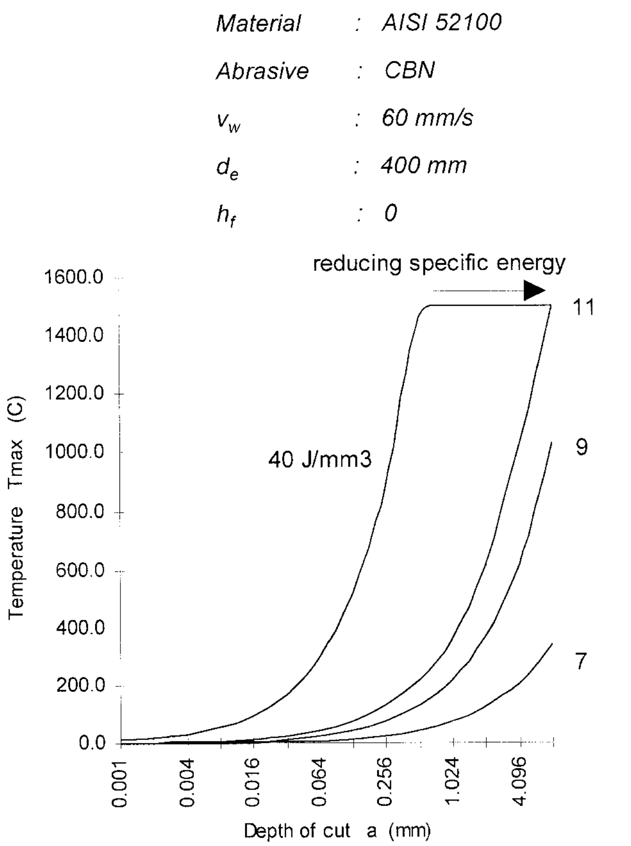

Fig. 12 Proposed explanation for HEDG based on the sliding model. Under HEDG conditions, contact temperatures are limited to the melting temperatures of the workpiece material. The energy is concentrated in a very thin layer. Specific energy is reduced because the shear forces are reduced

reduced. It is suggested that it is the drastic reduction in heat generated which makes HEDG possible.

The fact that it is possible to carry out these calculations based on heat transfer does not necessarily mean that such conditions are readily achieved in practice. However, commercial machines are available for the HEDG process and the process is carried out in industry so it is time to explain the physics of the process.

As illustrated in Fig. 12 maximum temperatures are increased as depth of cut is increased. At high temperatures in shallow grinding, large flows of energy take place within a short contact region. This concentration of energy softens the workpiece below the surface and causes thermal expansion, often leading to metal loading of the grinding wheel and surging power levels. The result is disastrous for precision grinding since the surface becomes very rough and the grinding wheel loses form.

Given this background of experience in shallow grinding, the question arises as to why HEDG is possible. A possible explanation is that, as workspeed and depth of cut are increased simultaneously, thermal expansions are less significant owing to the already large depths of cut. It is therefore possible under the right conditions to approach melting temperature, greatly reducing the specific energy so that a reduced quantity of heat is concentrated in a thin layer at the contact surface as illustrated in Fig. 12.

The high wheel speeds assist in maintaining the high contact temperatures and the rapid removal of the softened layer. High work speeds are essential to prevent excessive conduction of heat down to the level of the finished workpiece surface.

When HEDG conditions are achieved, the increases in specific removal rate are spectacular. Figure 13 shows the specific removal rates corresponding to Fig. 12. At the depth of cut of 8.2 mm, the specific removal rate is 492 mm^2/s compared with conventional values of the order of 3 mm^2/s, an increase of 2 orders of magnitude.

For lower specific removal rates, $Q'_w < 20\,mm^2/s$, and for the highest specific removal rates, $Q'_w > 70\,mm^2/s$, Tawakoli recommends down-grinding to obtain lower

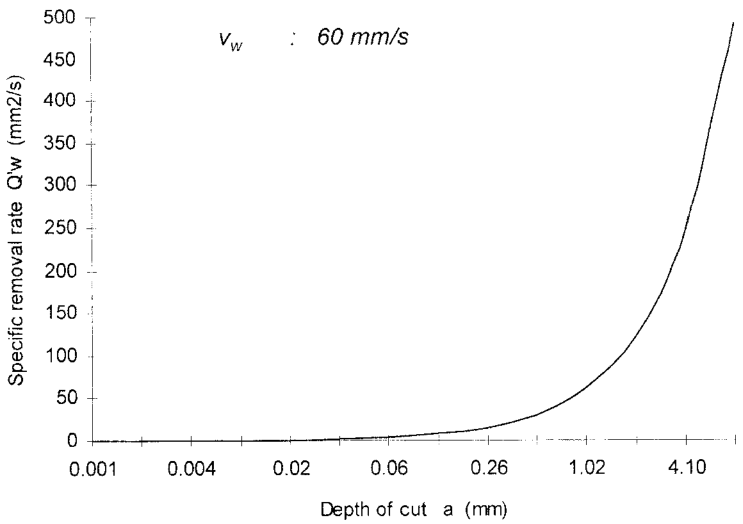

Fig. 13 Specific removal rate against depth of cut

forces and less wheel wear. For intermediate values, Tawakoli recommends up-grinding to reduce thermal damage. These recommendations can be interpreted in the light of the thermal analysis as follows. Up-grinding gives lower temperatures for the intermediate values because this is the condition where convective cooling is effective. Up-grinding may allow the fluid to act on more than half the arc of contact before boiling occurs. In down-grinding, the temperatures where the fluid enters the contact zone are higher and burn-out occurs within a short arc of contact so that convection is less effective.

For smaller depths of cut and lower removal rates, the conditions are similar to conventional grinding and fluid cooling is secondary to the importance of forces and wheel wear on the rate of heat generation. For the highest removal rates in HEDG, fluid convection again becomes secondary to the importance of reducing forces and wheel wear. Down-grinding is therefore employed which imparts higher fracture forces on the abrasive grits/bond bridges and helps to maintain cutting efficiency. This is consistent with the hypothesis that under these conditions HEDG operates as a dry grinding process.

9 DIRECT APPLICATION OF FIG. 7

To apply the data in Fig. 7, the user needs to know the heat flux, q_w, which depends on the partition ratio, R_w. A simplified approach is first to estimate T_{max} from equation (25) based on the sliding model. This allows the flux convected by the fluid, q_w, to be estimated using equation (20). A first estimate of R_w can be obtained from

$$R_w = R_{ws} - \frac{q_{ch}}{q_t} - \frac{q_f}{q_t} \qquad (28)$$

The heat entering the workpiece, $q_w = R_w q_t$, can then be used with Fig. 7 to obtain a more accurate value of T_{max}. If necessary the procedure can be repeated to achieve more accurate values of R_w and T_{max}. This also allows the maximum temperature on the finished workpiece surface to be estimated.

10 CONCLUSIONS

The physics of the grinding process are dependent on the heat transfer conditions and the kinematics of the process. Under deep grinding conditions at high work speeds, the maximum background temperature on the contact surface is reduced by the inclination angle of the moving heat source. The inclined heat source therefore gives more accurate predictions of temperatures than the sliding source model. Both models suffer from errors because the workpiece surface is non-planar. However, the inclined heat source model provides insights which are not available from the sliding source model. Further refinement of the model will allow account to be taken of the effects of the non-planar surface in making temperature estimates.

HEDG introduces a new physical limitation on the process which is that the maximum temperature cannot exceed a temperature approaching the melting temperature of the workpiece material. This potentially creates a limitation on the maximum specific energy in HEDG. In creep grinding with deep cuts, fluid convection usually predominates. In HEDG burn-out may occur and conduction predominate.

It has been shown that convection by the chips, the abrasive grains and the process fluid can all be important depending on the grinding domain. A methodology has been presented to estimate maximum temperatures across the range of grinding domains.

ACKNOWLEDGEMENTS

Particular thanks are due to Dr M. Morgan, Dr S. Black, Dr X. Chen and D. McCormack, and also to EPSRC, Universal Grinding Wheel Company, De Beers, British Steel, Lucas and Castrol for support of related projects which underpinned this work.

REFERENCES

1 **Carslaw, H.** and **Jaeger, J. C.** *Conduction of Heat in Solids*, Oxford Science Publications, 1959 (Oxford University Press, Oxford).

2 **Outwater, J. O.** and **Shaw, M. C.** Surface temperatures in grinding. *Trans. ASME*, 1952, **74**, 73–78.

3 **Hahn, R. S.** On the nature of the grinding process. In Proceedings of Third Machine Tool Design and Research Conference, 1962, pp. 129–154.

4 **Makino, Suto** and **Fokushima** An experimental investigation of the grinding process. *J. Mech. Lab. Japan*, 1966, **12**(1), 17.

5 **Des Ruisseaux, N. R.** and **Zerkle, R. D.** Temperatures in semi-infinite and cylindrical bodies subject to moving heat sources and surface cooling. *J. Heat Transfer*, 1970, **92**, 456–464.

6 **Malkin, S.** and **Cook, N. H.** The wear of grinding wheels, part 2—fracture wear. *Trans. ASME, J. Engng for Industry*, November 1971, **93**, 1129–1133.

7 **Shafto, G. R.** Creep-feed grinding. PhD thesis, University of Bristol, 1975.

8 **Snoeys, R., Maris, M.** and **Peters, J.** Thermally induced damage in grinding. *Ann. CIRP*, 1978, **27**(2), 571–581.

9 **Werner, P. G., Younis, M. A.** and **Schlingensiepen, R.** Creep-feed—an effective method to reduce workpiece surface temperatures in high efficiency grinding processes. In Proceedings of 8th SME North American Metalworking Research Conference, 1980, pp. 312–319 (Society of Manufacturing Engineers).

10 **Lavine, A. S.** Thermal aspects of grinding: heat transfer to workpiece wheel and fluid. Collected papers in heat transfer. *Trans. ASME, Heat Transfer Division*, 1989, **123**, 267–274.

11 **Rowe, W. B., Morgan, M. N.** and **Allanson, D. R.** An advance in the thermal modelling of thermal effects in grinding. *Ann. CIRP*, 1991, **40**(1), 339–342.
12 **Rowe, W. B., Qi, H. S., Morgan, M. N.** and **Zhang, H. W.** The effect of deformation in the contact area in grinding. *Ann. CIRP*, 1993, **42**(1), 409–412.
13 **Rowe, W. B., Black, S. C. E., Mills, B., Qi, H. S.** and **Morgan, M. N.** Experimental investigation of heat transfer in grinding. *Ann. CIRP*, 1995, **44**(1), 329–332.
14 **Ueda, T., Sato, M.** and **Nakayama, K.** Cooling characteristics of the cutting grains in grinding. *Ann. CIRP*, 1996, **45**(1), 293–298.
15 **Rowe, W. B., Black, S. C. E., Mills, B.** and **Qi, H. S.** Analysis of grinding temperatures by energy partitioning. *Proc. Instn Mech. Engrs, Part B, Journal of Engineering Manufacture*, 1996, **210**(B6), 579–588.
16 **Howes, T. D., Neailey, K.** and **Harrison, A. J.** Fluid film boiling in shallow cut grinding. *Ann. CIRP*, 1987, **36**(1), 223–226.
17 **Rowe, W. B., Pettit, J. A., Boyle, A.** and **Moruzzi, J. L.** Avoidance of thermal damage in grinding and prediction of the damage threshold. *Ann. CIRP*, 1988, **37**(1), 327–330.
18 **Rowe, W. B., Black, S., Mills, B., Morgan, M.** and **Qi, H. S.** Grinding temperatures and energy partitioning. *Proc. R. Soc. Lond., Part A*, 1997, **453**, 1083–1104.
19 **Morgan, M. N., Rowe, W. B., Black, S. C. E.** and **Allanson, D. R.** Effective thermal properties of grinding wheels and grains. *Proc. Instn Mech. Engrs, Part B, Journal of Engineering Manufacture*, 1998, **212**(B8), 661–669.
20 **Andrew, C., Howes, T.** and **Pearce, T.** *Creep-Feed Grinding*, 1985 (Rinehart and Winston, New York).
21 **Rowe, W. B., Morgan, M. N., Black, S. C. E.** and **Mills, B.** A simplified approach to thermal damage in grinding. *Ann. CIRP*, 1996, **45**(1), 299–302.
22 **Lee, D. G., Zerkle, R. D.** and **Des Ruisseaux, N. R.** An experimental study of thermal aspects of cylindrical grinding. ASME paper WA-71/Prod-4, 1971.
23 **Tawakoli, T.** *High Efficiency Deep Grinding*, 1993 (VDI-Verlag and Mechanical Engineering Publications).
24 **Guhring, K.** Hochleistungs-schleifen. Dissertation, RWTH, Aachen, 1967.